

# SUPER-RESOLUTION WITH ADAPTIVE REGULARIZATION

A. Lorette\* H. Shekarforoush\*\* J. Zerubia\*

\*INRIA-2004 Route des Lucioles  
BP 93  
06902 Sophia Antipolis Cedex  
France

\*\*Center For Automation Research  
University of Maryland  
College Park, MD 20742  
U.S.A.

## ABSTRACT

*Multi-channel super-resolution is a means of recovering high frequency information by trading off the temporal bandwidth. Almost all the methods proposed in the literature are based on optimizing a cost function. But since the problem is usually ill-posed, one needs to impose some regularity constraints. However, regularity constraints tend to attenuate high frequency contents of data (usually present in the form of discontinuities). This inherent contradiction between regularization and super-resolution has not been addressed in the literature, despite the availability of off the shelf tools. In this paper, we have investigated this issue in the context of adaptive regularization, using  $\phi$ -functions (convex, non-convex, bounded, unbounded).*

## 1. INTRODUCTION

Except for the very first publication on multi-channel super-resolution [1], all other works on this subject [2][3][4] have been based on optimizing a cost function under regularity constraints<sup>1</sup>(see also [5] for more references). Ironically, regularity constraints tend to attenuate the high frequency information, which is exactly what super-resolution methods attempt to recover. This inherent contradiction between regularization and super-resolution has not been addressed in the existing literature. In this work, we have therefore studied the possibility of overcoming this contradiction, using an adaptive regularization. A comparative view of different prior models has been provided.

## 2. DATA MODEL

Our imaging model is as in [4]: each low resolution image is obtained from a 3D scene through uncorrelated

\*\*The second autor was at INRIA-Sophia Antipolis when this research was carried out.

<sup>1</sup>Note that, in this paper we are only interested in multi-channel methods and single-channel methods will not be considered.

channels (here, uncorrelated implies that inter-frame shifts are of sub-pixel order), including noise, blur and sub-sampling:

$$I(k, l) = \sum_{(i, j) \in W} g(i, j) R(i, j) h(i - i_o, j - j_o) \quad (1)$$

where  $g$  is the scene albedo at high resolution coordinates  $(i, j)$ ,  $R$  is the reflectance map,  $h$  is the Point Spread Function (PSF) of the camera assumed linear and invariant to any arbitrary shift  $(i_o, j_o)$  in a compact support  $W$  and  $I$  is the observed image intensity at low resolution coordinates  $(k, l)$ .

We will assume that  $m$  low resolution images are available. We will use Markov Random Fields (MRF) for modelling the albedo and the altitude, where the MRF associated with the albedo will be denoted by  $G$  and the one associated with the altitude by  $Z$ .  $G$  and  $Z$  will be assumed to be independent. We will also denote our low resolution image sequence by  $I_1, \dots, I_m$ . These are assumed to be degraded by three factors: a white Gaussian noise of variance  $\sigma_e$ , the PSF of the camera  $h$  (acting as a low-pass filter) and sub-sampling. The problem is to find the best estimator of  $G$  or  $Z$  at a higher resolution (ie. higher sampling density), using the low resolution sequence  $I_1, \dots, I_m$ .

The method proposed herein, is based on a Bayesian framework and the MAP criterion. Therefore, we need to maximize the following probability density:

$$P(G, Z | I_1, \dots, I_m) = P(I_1, \dots, I_m | G, Z) * P(G, Z) \quad (2)$$

where  $P(I_1, \dots, I_m | G, Z)$  and  $P(G, Z)$  are the conditional and the prior densities, respectively. Since, we have made the assumption that the sequence  $I_1, \dots, I_m$  is obtained by uncorrelated channels:

$$P(I_1, \dots, I_m | G, Z) = \prod_{r=1}^m \frac{1}{\sigma_e^2} \exp \left\{ -\frac{\|I_r - \hat{I}_r\|^2}{2\sigma_e^2} \right\} \quad (3)$$

where  $\hat{I}_r$ 's represent the estimated low resolution images, obtained by simulating the imaging process in (1) from some estimated albedo and altitude. Recall that, for our problem, we have assumed that  $h$  is known so that the imaging process can be simulated from any initial estimate of the albedo and the altitude at high resolution.

Notice that the imaging equation (1) is linear with respect to  $g$  but rather non-linear with respect to the altitude (appearing in  $R(i, j)$  [6]). Therefore, in order to simplify the problem at this stage, we will assume that the altitude is known. Therefore, the cost function to be minimized will be as follows:

$$\begin{aligned}
E = & \sum_{i,j} \left( \sum_{r=1}^m \sum_{(k,l) \in \nu_r(i,j)} \frac{(\hat{I}^r(k,l) - I^r(k,l))^2}{2\sigma_e^2} \right. \\
& + \sum_{(i',j') \in V(i,j)} \frac{\phi\left(\frac{g(i,j) - g(i',j')}{\Delta_g}\right)}{2\sigma_g^2} \\
& \left. + \sum_{(i',j') \in V(i,j)} \frac{\phi\left(\frac{z(i,j) - z(i',j')}{\Delta_z}\right)}{2\sigma_z^2} \right) \quad (4)
\end{aligned}$$

where  $\nu_r(i, j)$  is the set of all pixels in the low resolution image  $r$ , whose intensity depends on the pixel  $(i, j)$  in the high resolution albedo and altitude,  $V(i, j)$  is the neighbourhood of pixel  $(i, j)$  (we have only used first order MRF's and two-sites cliques.) and  $\Delta_g$  and  $\Delta_z$  are scale parameters which characterize the minimal height of discontinuities that we wish to preserve.

### 3. PRIOR MODEL

Since our objective is to recover high frequency information by data fusion (ie. increase the sampling density using an image sequence), it would seem natural to attempt preserving discontinuities (ie. those image features that carry high frequency information). Therefore, our prior model can not be the standard Tikhonov-Arsenin stabilizing functionals which tend to over-smooth data. We have used three different potential functions given below in equations (5) (6) and (7) (proposed, respectively, by Charbonnier [7], Hebert-Leahy [8], and Geman-et al. [9]):

$$\phi(u) = 2 * \sqrt{1 + u^2} - 2 \quad (5)$$

$$\phi(u) = \log(1 + u^2) \quad (6)$$

$$\phi(u) = \frac{u^2}{1 + u^2} \quad (7)$$

Note that these three functions are even, monotonically increasing and quadratic around the origin (see Figure 1).

For the a priori we will limit the approximation to order 1. In other words, we will only take into account first order differences for the neighbouring pixels. One can always attempt higher order approximations at the cost of further complexity.

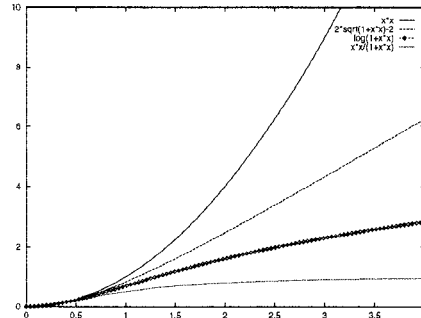


Figure 1: Different  $\phi$ -functions; from top to bottom: standard quadratic, functions in (5), (6) and (7)

### 4. ALGORITHMIC ASPECTS

The algorithm is based on minimizing the cost function in (4) with respect to  $g$  (recall that we have assumed that both the altitude and the camera PSF are known). Therefore, the cost function can be evaluated for any given estimate. This implies that one may apply iterative optimization methods for reconstructing the high resolution albedo.

Different optimization methods were used for each prior model proposed above: for the function in (5), we applied Newton's deterministic method, for the one in (6) the simulated annealing and for the last function a deterministic algorithm called ARTUR (proposed originally by Charbonnier-et al. [10] in tomographic reconstruction). The later uses continuous auxiliary variables and alternates between these variables and the main variable (ie.  $g$  in our case).

As for the first two models, the algorithm was initialized with random images. Since, for the first function, the resulting cost function is convex, we used Newton's method. This, however, was not the case for the second function, and hence Simulated Annealing (SA) was applied. For the last model, we used the deterministic algorithm ARTUR, despite the non-convexity of the cost function. Therefore, the algorithm had to be initialized near the solution (using for example interpolated versions of the input data). As a

comparison, we noticed that, for the last function, the chances of falling into local minima were noticed to be quite high (even if we used SA).

### 5. RESULTS

Compared to the standard quadratic regularization (see Figures 2 and 6), we observe an improvement with the adaptive regularization. This remark remains valid for both synthetic and real data.

However, the difference between the three  $\phi$ -functions only stands out, when the input images are of different natures. Theoretically, the unbounded non convex  $\phi$ -function in (7) should give the best result, since it penalizes less the high gradient values. However, in practice, this is not necessarily the case. We have observed a clear improvement of the results on the synthetic images with both non-convex models in (6) (see Figure 4) and (7) (see Figure 5) compared to those obtained with the convex one (see Figure 3). However, this remark does not hold anymore for real images. In fact, for real data, all the three models (see Figures 7, 8 and 9) gave similar results with slightly better results for the unbounded non-convex  $\phi$ -function in (6) (see Figure 7).

An explanation for the above observations is as follows:

The synthetic images are piecewise constant. Thus, a first order approximation is well adapted, independently of the  $\phi$ -function. However, for real images (which are not in general piecewise constant), a first order approximation with the non-convex  $\phi$ -functions does not yield better results than the convex one. The best results are obtained with the non convex  $\phi$ -function in (6) when used together with the SA. In the case of real data the best compromise between the computational time and the quality of the results is, to our opinion, obtained with the convex  $\phi$ -function. Therefore, the optimization aspects need to be reviewed in depth.

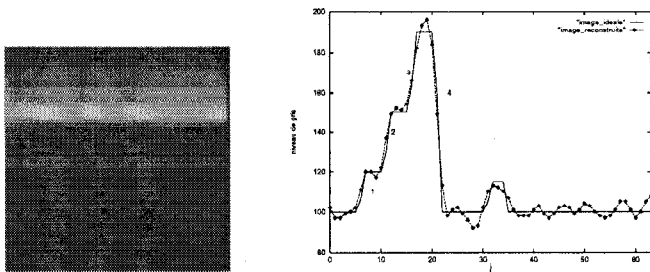


Figure 2: reconstructed image and a profile (SNR=44.7 dB)

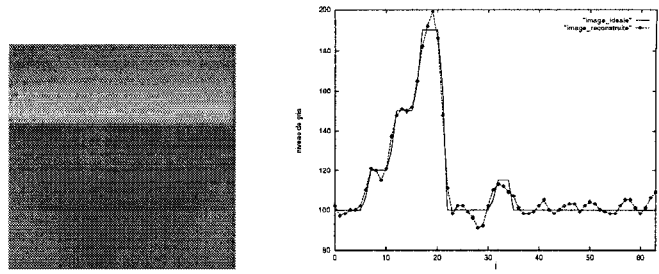


Figure 3: reconstructed image and a profile (SNR=46.3 dB)

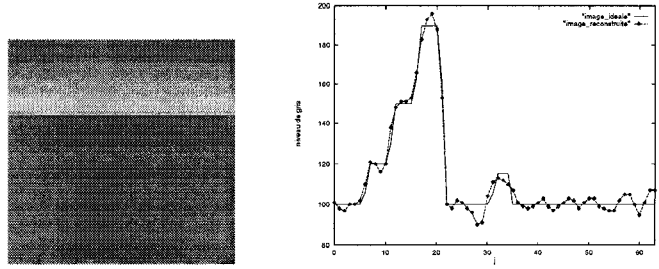


Figure 4: reconstructed image and a profile (SNR=49 dB)

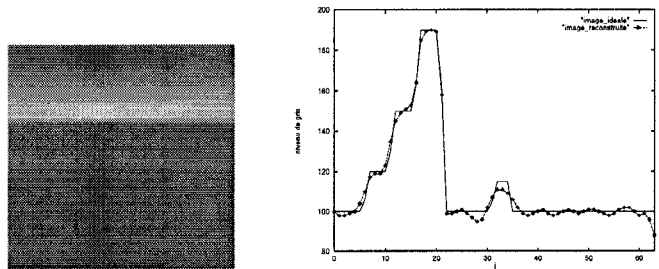


Figure 5: reconstructed image and a profile (SNR=53.4 dB)

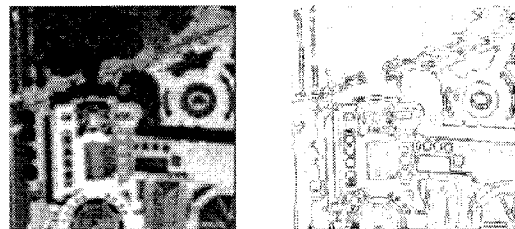


Figure 6: reconstructed image and error image for a classical gaussian regularization (SNR=34.5 dB)

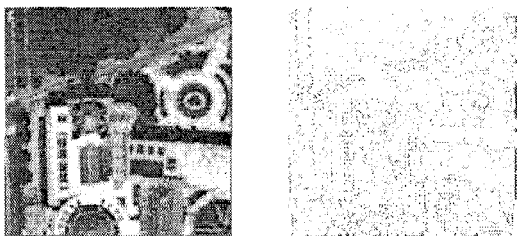


Figure 7: reconstructed image and error image for the convex prior model (SNR=37 dB)

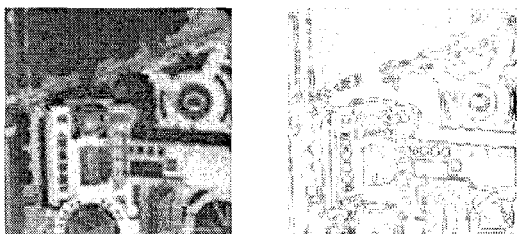


Figure 8: reconstructed image and error image for the nonconvex, bounded prior model (SNR=36.9 dB)

## 6. CONCLUSION

The aim of this work was to study the possibility of overcoming the contradictory nature between super-resolution and regularization, using off the shelf tools. We have shown that, it would be possible to improve the performance of super-resolution algorithms by using an adaptive regularization, which would allow for preserving discontinuities (ie. high frequency information). We have also provided a comparative study of different adaptive models as against to the classical quadratic regularization, which tends to over-smooth discontinuities.

Our study shows that first order approximation is not well adapted for real data in the context of super-resolution and adaptive regularization. Obviously the choice of an adequate optimization method is also of great importance, so that the performance of non-convex models can stand out. Perhaps, from a purely optimization point of view, one could resort to multi-scale methods or other optimization methods (eg. zero order search methods like the one proposed in [11]).

## 7. REFERENCES

[1] R. Y. Tsai and T. S. Huang. Multiframe image restoration and registration. *ACVIP*, 1:317–339, 1984.

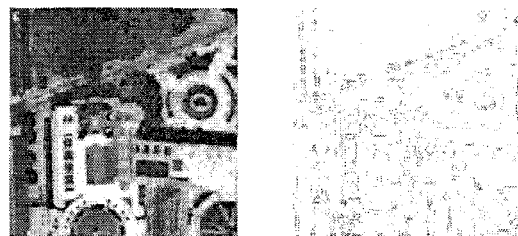


Figure 9: reconstructed image and error image for the nonconvex, non bounded prior model (SNR=37.8 dB)

[2] M. Irani and S. Peleg. Improving resolution by image registration. *CVGIP*, 53(3):231–239, May 1991.

[3] H. Ur and D. Gross. Improved resolution from subpixel shifted pictures. *CVGIP*, 54(2):181–186, March 1992.

[4] H. Shekarforoush, M. Berthod, J. Zerubia, and M. Werman. Sub-pixel bayesian estimation of albedo and height. *IJCV*, 3(19):289–300, 1996.

[5] H. Shekarforoush. *Super-resolution in computer vision*. PhD thesis, (in English), UNSA, November 1996.

[6] M. Berthod, H. Shekarforoush, M. Werman, and J. Zerubia. Reconstruction of high resolution 3d visual information. In *CVPR*, pages 654–657, Seattle, June 1994.

[7] P. Charbonnier. *Reconstruction d'image: régularisation avec prise en compte des discontinuités*. PhD thesis, (in French), UNSA, September 1994.

[8] T. Hebert and R. Leahy. A generalized em algorithm for 3d bayesian reconstruction from poisson data using gibbs priors. *IEEE Trans. Med. Imaging*, MI-8:194–202, June 1989.

[9] D. Geman and G. Reynolds. Constrained restoration and the recovery of discontinuities. *IEEE Trans.*, PAMI-14(3):367–383, March 1992.

[10] P. Charbonnier, L. Blanc-Féraud, G. Aubert, and M. Barlaud. Two deterministic half quadratic regularization algorithms for computed imaging. In *ICIP*, pages 168–171, November 1994.

[11] H. Shekarforoush, M. Berthod, and J. Zerubia. A generalization of the non-linear simplex search method. In *SIAM*, Victoria, British Columbia, 1996.